

Modeling and Analysis of Uplink Non-Orthogonal Multiple Access (NOMA) in Large-Scale Cellular Networks Using Poisson Cluster Processes

Hina Tabassum, Ekram Hossain, and Md. Jahangir Hossain

Abstract

Non-orthogonal multiple access (NOMA) serves multiple users by superposing their distinct message signals. The desired message signal is decoded at the receiver by applying successive interference cancellation (SIC). Using the theory of Poisson cluster process (PCP), this paper provides a framework to analyze multi-cell uplink NOMA systems. Specifically, we characterize the rate coverage probability of a NOMA user who is at rank m (in terms of the distance from its serving BS) among all users in a cell and the mean rate coverage probability of all users in a cell. Since the signal-to-interference-plus-noise ratio (SINR) of m -th user relies on efficient SIC, we consider three scenarios, i.e., perfect SIC (in which the signals of $m - 1$ interferers who are stronger than m -th user are decoded successfully), imperfect SIC (in which the signals of $m - 1$ interferers who are stronger than m -th user may or may not be decoded successfully), and imperfect worst case SIC (in which the decoding of the signal of m -th user is always unsuccessful whenever the decoding of its relative $m - 1$ stronger users is unsuccessful). The worst case SIC assumption provides remarkable simplifications in the mathematical analysis and is found to be highly accurate for scenarios of practical interest. To analyze the rate coverage expressions, we first characterize the Laplace transforms of the intra-cluster interferences in closed-form considering both perfect and imperfect SIC scenarios. In the sequel, we characterize the distribution of the distance of a user at rank m which is shown to be the generalized Beta distribution of first kind and the conditional distribution of the distance of the intra-cluster interferers which is different for both perfect and imperfect SIC scenarios. The Laplace transform of the inter-cluster interference is then characterized by exploiting distance distributions from geometric probability. The derived expressions are customized to capture the performance of a user at rank m in an equivalent orthogonal multiple access (OMA) system. Finally, numerical results are presented to validate the derived expressions. It is shown that the average rate coverage of a NOMA cluster outperforms its counterpart OMA cluster with higher number of users per cell and higher target rate requirements. A comparison of Poisson Point Process (PPP)-based and PCP-based modeling is conducted which shows that the PPP-based modeling provides optimistic results for the NOMA systems.

Index Terms

H. Tabassum and E. Hossain are with the Department of Electrical and Computer Engineering at the University of Manitoba, Canada. Md. J. Hossain is with the University of British Columbia (Okanagan Campus), Canada.

Matern cluster process, multi-cell uplink NOMA, rate coverage probability, order statistics.

I. INTRODUCTION

Until very recently, the state-of-the-art wireless communications systems have been utilizing a variety of orthogonal multiple access (OMA) technologies, in which the resources are allocated orthogonally to multiple users. These techniques include frequency-division multiple access (FDMA), time-division multiple access (TDMA), code-division multiple access (CDMA), and orthogonal frequency-division multiple access (OFDMA). Since OMA maintains the orthogonality among users in a cell, the intra-cell interference (i.e., inter-user interference within a cell) does not exist. As a result, the information signals of users can be retrieved at a low complexity. Nonetheless, the number of served users is limited by the number of orthogonal resources.

Conversely, NOMA serves multiple users simultaneously using the same spectrum resources (i.e., radio channels), however, at the cost of increased intra-cell interferences. To mitigate the intra-cell interferences, NOMA exploits Successive Interference Cancellation (SIC) at the receivers [1]. NOMA supports low transmission latency and signaling cost compared to conventional OMA where each user is obliged to send a channel scheduling request to its serving base station (BS). With these attractive features, NOMA can be a potential access technology for 5G networks. Nevertheless, the conclusions about the performance of NOMA are largely unknown in multi-cell network scenarios. For instance, in uplink NOMA, a large number of transmitting users in the neighboring co-channel BSs can result in high interference at the BS of interest. Consequently, the uplink multi-cell interference in NOMA is directly proportional to the number of transmitting users per neighboring co-channel BS and is more severe compared to the inter-cell interference in OMA.

A. Background Work

The concept of NOMA was initially proposed in [1] for downlink transmissions. Various practical aspects, such as multi-user scheduling, impact of error propagation in SIC, overall system overhead, and user mobility were discussed. System level simulations were conducted in [2] to highlight the benefits of two-user NOMA over OMA, in terms of overall system throughput as well as individual user's throughput.

The approximate expressions for the ergodic sum-rate and outage probability of a user in a given downlink NOMA cluster were derived in [3]. Later, in [4], the throughput gains of the two-user cooperative NOMA (in which the strong channel user relays the information of weak channel user) were investigated. The idea of cooperative NOMA was then applied to wireless-powered systems in [5]. Based on users' distances, grouping of users was performed first. Then, three user selection schemes were investigated,

i.e., (i) pairing of the nearest users from each group, (ii) pairing of the nearest user from one group and the farthest user from another group, and (iii) arbitrary user pairing. The direct link was used to transfer energy from the BS. A cooperative data link was established for the lower channel gain user via the higher channel gain users. Closed-form approximate expressions for the outage probability and throughput of a two-user NOMA cluster were derived. In [6], the user pairing was investigated considering fixed NOMA (F-NOMA) and cognitive radio inspired (CR-NOMA). In F-NOMA, any two users could make a NOMA pair based on their channel gains. While in CR-NOMA, a weak channel user opportunistically gets paired with the strong channel user provided that the interference caused by the strong user will not harm the rate requirement of the weak channel user. It was observed that CR-NOMA pairs the strongest user with the second strongest user, whereas F-NOMA pairs a strongest user with the weakest user in the system.

A general concept of uplink NOMA was discussed in [7]. An uplink power back-off policy was proposed to distinguish users in a NOMA cluster with nearly similar signal strengths (given that traditional uplink power control is applied). Closed-form analysis was performed for ergodic sum-rate and outage probability of a two-user NOMA cluster. Further, the problem of user scheduling, subcarrier allocation, and power control in uplink NOMA has been investigated by various researchers in [8], [9] with perfect SIC at the BS. A game theoretic algorithm for uplink power control has been designed in [10] considering a two-cell NOMA system where inter-cell interference is assumed to be Gaussian distributed.

B. Motivations and Contributions

To date, most of the research investigations consider the throughput analysis of NOMA for single-cell downlink systems with perfect SIC at the receivers. The derived expressions generally leverage on high signal-to-noise ratio (SNR) and asymptotic assumptions as well as the application of Gaussian-Chebyshev quadrature (GCQ) technique which approximates all integrals into finite sums. Unfortunately, the conclusions about the performance gains of NOMA (compared to OMA) in single-cell/single-cluster scenarios cannot be applied directly to multi-cell/multi-cluster scenarios. The reason is the inter-cell¹ interferences in NOMA can be quite severe as well as distinct from OMA, especially in the uplink scenarios [11]. Note that, in uplink NOMA, the inter-cell interference incurred at the BS of interest is directly proportional to the number of transmitting users in neighboring co-channel BSs. This is different from an equivalent uplink OMA system where only one user transmits at a time per neighboring co-channel BS.

Further, compared to downlink NOMA, we note that the performance analysis of uplink NOMA is particularly more challenging due to the mathematical structure of the intra-cell interferences. In the uplink

¹The term inter/intra-cell and inter/intra-cluster interference will be used interchangeably throughout the paper.

NOMA, the BS receives transmissions from all users simultaneously. As such, the intra-cell interference to a user is a function of the channel statistics of other users within the cell. On the other hand, in downlink NOMA, the intra-cell interference to a user is a function of its own channel statistics [3], [4], [6]. To this end, the contributions of this paper are outlined as follows:

- Using the theory of order statistics and Poisson Cluster Process² (PCP), we develop a framework to analyze the rate coverage probability of a user who is at rank m (in terms of the distance from its serving BS) among all users in a cell and the mean rate coverage probability of all users in a cell, considering a multi-cell uplink NOMA system. Unlike typical stochastic geometry frameworks where the user locations are uniform over the 2-D plane and are independent of the BS locations [17], [18], we exploit Matern Cluster Process (MCP) to accurately model the proximity of multiple users around a BS³.
- NOMA systems rely on efficient SIC and the interference of a user at rank m needs to be adapted according to the level of SIC. We consider three SIC scenarios that include perfect SIC (in which the signals of $m-1$ interferers who are stronger than m -th user are decoded successfully), imperfect SIC (in which the signals of $m-1$ interferers who are stronger than m -th user may or may not be decoded successfully), and imperfect worst case SIC (in which the decoding of the signal of m -th user is always unsuccessful whenever the decoding of its relative $m-1$ stronger users is unsuccessful). The worst case SIC assumption provides remarkable simplifications in the mathematical analysis and is found to be highly accurate for scenarios of practical interest.
- The interference power at the BS of a given cell/cluster is composed of intra-cluster and inter-cluster interferences. We derive the Laplace transform of the intra-cluster interference in closed-form considering various SIC scenarios. In the sequel, we also derive the distribution for the distance of a user at rank m which is shown to be the generalized Beta distribution of first kind and the conditional distribution of the distance of the intra-cluster interferers which is different for both perfect and imperfect SIC scenarios. The Laplace transform of the inter-cluster interference is then characterized using distance distributions from geometric probability. A less-complex bound is then exploited to model the Laplace transform of the inter-cluster interference.
- The derived rate coverage expressions are customized to evaluate the performance of a user at rank m in an equivalent OMA system in closed-form. Numerical results are presented to validate the

²Neyman-Scott PCP, such as Modified Thomas Cluster process and Matern Cluster Process, are recently exploited in a set of research studies for performance evaluation of ad-hoc clustered networks [12], D2D systems [13], [14], and downlink multi-tier cellular networks [15], [16].

³The Poisson Point Process (PPP)-based modeling of BSs and user devices focuses on the link between the serving BS and a typical user. Since the typical user can be located anywhere in the cell, results are averaged over all spatial positions inside the cell. Such an approach provides higher analytical flexibility. However, in practice, users are more likely clustered around a BS and are distinct due to their channel conditions. In this regard, PCP have been shown empirically to be a more accurate cellular network modeling technique [19] that allows location-specific performance modeling of users.

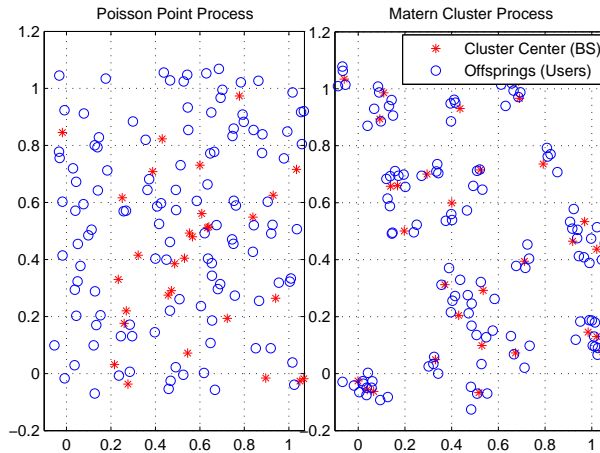


Fig. 1: Graphical illustration of the single-tier cellular network with (a) conventional PPP model and (b) Matern Cluster Process (MCP) model in which the number of users are Poisson distributed and their locations are uniformly distributed within a disc of radius R per cluster center.

derived expressions. Our results indicate that the performance benefit of OMA diminishes quickly with the increase in number of users per cluster and higher user rate requirements. A comparative performance analysis of PPP-based and PCP-based modeling is conducted using simulations. It is shown that PPP-based modeling generally provides optimistic results for the NOMA systems due to the homogeneous distribution of users regardless of the BS locations which reduces the impact of intra-cluster interference.

The rest of the paper is structured as follows. Section II discusses the working principle of uplink NOMA along with cellular network model, channel model, and interference model. In Section III, we describe the fundamental differences between conventional SIC and SIC for NOMA. Considering perfect SIC, imperfect SIC, and imperfect worst case SIC, we model the interferences and define the desired performance metrics. In Section IV, we derive relevant distance distributions required for the characterization of the Laplace transforms of the interferences. In Section V, we derive the rate coverage expressions for both NOMA and OMA systems. Finally, Section VI discusses numerical and simulation results followed by the concluding remarks in Section VII.

II. SYSTEM MODEL AND ASSUMPTIONS

A. Spatial Cellular Network Model

We consider a single-tier cellular network composed of macrocell base stations (BSs) surrounded by user devices. The locations of transmitting user devices are modeled as a stationary and isotropic PCP.

Definition 1 (Poisson Cluster Process (PCP) [12]). *A PCP results from applying homogeneous independent clustering to a stationary Poisson Point Process (PPP). In particular, the parent points form a stationary*

PPP $\phi = \{x_1, x_2, \dots\}$ of density λ . The off-springs N^{x_i} generated for a given parent x_i are a family of independent and identically distributed (i.i.d.) finite point sets with distribution independent of the parent process. The complete PCP can thus be represented as $\Xi = \bigcup_{x \in \Phi} N^x$. Note that the parent points themselves will not be included in the PCP. The parents and off-springs are referred to as the cluster centers and the cluster members, respectively.

Definition 2 (Neyman-Scott PCP). *If the number of points per cluster follow a Poisson distribution with mean intensity \bar{c} , such a PCP is referred to as a Neyman-Scott Process.*

MCP is a special case of the Neyman-Scott PCP where the cluster centers (BSs) are modeled by a parent homogeneous PPP $\Phi_m = \{x_0, x_1, x_2, \dots\}$ in the Euclidean plane with density λ_m . Each parent point $x_i \in \Phi_m$ forms the center of a cluster around which daughter points (user devices) are uniformly distributed in a circle of radius R as shown in Fig. 1. For ease of exposition, we consider \bar{c} number of users per cluster. Each daughter point located at y with respect to its cluster center x_i has a density function as:

$$f(y) = \frac{1}{\pi R^2}, \quad \|y\| \leq R, \quad (1)$$

where $\|y\| = r$ is the distance of any arbitrary daughter point (user device) relative to its cluster center (serving BS) and its density function can be given as follows:

$$f(r) = \frac{2r}{R^2}, \quad r \leq R. \quad (2)$$

The resulting MCP is a stationary and isotropic point process of density $\bar{c}\lambda_m$ and can be defined as $\Xi = \bigcup_{x_i \in \Phi_m} \mathcal{N}^{x_i}$. Without loss of generality, we perform analysis for a user at rank m located in a randomly chosen cluster which is referred as representative cluster located at x_0 throughout the paper.

B. Working Principle of Uplink NOMA

In an uplink NOMA cluster, each user transmits its individual signal \hat{x}_i with a transmit power p_i such that the received signal at the BS can be defined as $\hat{y} = \sum_{i=1}^{\bar{c}} \sqrt{p_i} h_i \hat{x}_i$. Note that, to apply SIC and decode signals at the BS, it is crucial to maintain the distinctness of various signals superposed within \hat{y} . Since the channels of different users are different in the uplink, each message signal experiences distinct channel gain⁴. As a result, the received signal power corresponding to the strongest channel user is likely the strongest at the BS. Therefore, this signal is decoded first at the BS and experiences interference from all users in the cluster with relatively weaker channels. That is, the transmission of the highest channel

⁴The conventional uplink transmit power control (typically intended to equalize the received signal powers of users) may remove the channel distinctness and thus may not be feasible for uplink NOMA transmissions.

gain user experiences interference from all users within its cluster, whereas the transmission of the lowest channel gain user receives zero interference from the users in its cluster.

C. Channel and Interference Model

NOMA allows multiple users in a cluster to share the same resources by superposing their distinct message signals. All users are served on the same channel and time slot. All users/BSs are equipped with a single antenna. Within the representative cluster, any arbitrary user device located at $y \in \mathcal{N}^{x_0}$ with respect to its serving BS located at $x_0 \in \Phi_m$ transmits its individual signal with power P_u such that the superposed NOMA signal at the representative BS can be defined as follows:

$$S_0 = \sum_{y \in \mathcal{N}^{x_0}} S_y = \sum_{y \in \mathcal{N}^{x_0}} P_u h_{y x_0} \|y\|^{-\alpha}, \quad (3)$$

where $\alpha > 2$ is the path-loss exponent and $h_{y x_0}$ is the exponential random variable which models Rayleigh fading associated with the channel between the node located at y and the BS located at x_0 . All fading coefficients are i.i.d. and the additive noise is complex Gaussian distributed with mean zero and variance $N_0/2$ per dimension.

Consequently, the uplink NOMA transmission of a user located at y_0 within the representative cluster is vulnerable to two kind of interferences, i.e.,

- *Intra-cluster interference*: is the interference received at the representative BS from all user devices located within the representative cluster (except the user located at y_0). However, after performing SIC, some of these interferences can be removed (details of SIC will follow in the next section).
- *Inter-cluster interference*: is the interference received at the representative BS from all user devices located outside the representative cluster.

Provided that the center of the representative cluster is located at $x_0 \in \Phi_m$, the intra-cluster interference experienced by the transmission of user located at y_0 with respect to its cluster center x_0 can be modeled as follows:

$$I_{\text{intra}} = \sum_{y \in \mathcal{N}^{x_0} \setminus y_0} P_u h_{y x_0} \|y\|^{-\alpha}. \quad (4)$$

Similarly, the inter-cluster interference at the representative BS from the user devices located outside the representative cluster center can be modeled as follows:

$$I_{\text{inter}} = \sum_{x \in \Phi_m \setminus x_0} \sum_{y \in \mathcal{N}^x} P_u h_{y x} \|x + y\|^{-\alpha}, \quad (5)$$

and $I_{\text{agg}} = I_{\text{intra}} + I_{\text{inter}}$. However, since NOMA systems rely on efficient SIC, the intra-cluster interference model needs to be adapted according to the level of SIC cancellations. This is elaborated in detail in the

next section.

III. SUCCESSIVE INTERFERENCE CANCELLATION (SIC) AND PERFORMANCE METRICS

In this section, we will discuss the fundamental differences between conventional SIC and SIC for NOMA. We then describe the signal-to-interference-plus-noise ratio (SINR) modeling with perfect and imperfect SIC in uplink NOMA. Considering three possible SIC scenarios, i.e., perfect SIC, imperfect SIC, and imperfect worst case SIC, we finally define the performance metrics.

SIC is among one of the best known interference cancellation methods as (i) the SIC receiver is architecturally similar to traditional non-SIC receivers in terms of hardware complexity and cost, (ii) it uses the traditional decoder to decode the composite signal at different stages and neither complicated decoders nor multiple antennas are required, and (iii) it can achieve the Shannon capacity for both the broadcast and multiple access networks [20], [21]. Typically, SIC is used to regenerate the interfering signals and subsequently cancel them from the received composite signal to improve the SINR of the desired signal. That is, the SIC receiver first decodes the strongest signal by treating other signals as noise. Then it regenerates the analog signal from the decoded signal and cancels it from the received composite signal. The remaining signal is thus free from the strongest interfering signal. Then, the SIC receiver proceeds to decode, regenerate, and cancel the second strongest interfering signal from the remaining signal and so on, until the desired signal can be decoded.

A. SIC and SIC Error Propagation in Uplink NOMA

In uplink NOMA, we apply the same SIC principle at the BS, i.e., the SIC receiver first decodes the strongest signal by treating other signals as noise and so on. However, the difference is that the intra-cluster interfering signals are also the desired signals; therefore, it is not possible to provide the benefits of SIC (enhance the SINR) unequivocally for all users. That is, within a cluster, the user with strongest signal experiences interference from all users and the user with the weakest signal enjoys zero intra-cluster interference. *Evidently, the intra-cluster interference statistics will vary for all user devices within the representative NOMA cluster.*

Since the decoding of the strongest signal is performed first at the BS, its success/failure has a significant impact on the decoding of other users' signals. Specifically, depending on the decoding result of the strongest signal, the interference used for the decoding of the second strongest signal differs, which makes the link-to-system mapping difficult. If the strongest signal is decoded correctly, its replica signal can be subtracted successfully from the superposed signal at the BS. Otherwise, the second strongest user will experience the interference from the strongest user as well as other users in the cluster. This phenomenon is referred to as SIC error propagation.

B. Modeling of Intra-cluster Interference with SIC

To model the intra-cluster interference with SIC, first the BS needs to rank the received powers of various users as $\{S_{(1)}, S_{(2)}, \dots, S_{(m)}, \dots, S_{(\bar{c})}\}$ such that $S_{(m)} \geq S_{(\bar{c})}$ with $m < \bar{c}$. However, note that the impact of path-loss factor is more stable and dominant compared to the instantaneous multi-path channel fading effects. Therefore, the order statistics of the distance outweigh the fading effects, which vary on a much shorter time scale. As such, the ranking of users in terms of their distances from the serving BS is generally considered as a reasonable approximate of their respective ranked received signal powers [22]. This approximation provides great flexibility for the analytical purposes. Also, the SIC based on long-term channel states is more practically feasible since it requires less overheads for channel estimation. Note that the exact performance analysis of the user with m^{th} strongest signal is unwieldy to solve since the distribution of $S_{(j)}$ is the ranked distribution of a composite uniform and exponential random variable and the joint distribution of several composite ordered random variables is required.

Approximation: As mentioned above, the impact of path-loss factor is more dominant compared to the channel fading effects. Hence, for tractability reasons, we assume that ordering of the received signal powers can be approximately achieved by ordering the distances of the users as $r_{(1)} \leq r_{(2)}, \dots, \leq r_{(m)}, \dots, \leq r_{(\bar{c})}$ such that $r_{(m)} \leq r_{(\bar{c})}$ with $m < \bar{c}$. That is, when the j -th strongest signal is decoded and subtracted from the composite signal, this means that the remaining interferers are located farther than the j -th rank user whose distance is $r_{(j)}$ from the representative BS.

The intra-cluster interference and in turn the SINR of m -th rank user can thus be modeled for perfect and imperfect SIC scenarios, respectively, as shown below.

1) *Perfect SIC:* In this case, a given user at rank m receives interferences from all users with relatively weaker channel gains (or users with farther distances as per the approximation) and the BS perfectly decodes/cancels the $m - 1$ strong interferences. The intra-cluster interference experienced by any user at m -th rank in a cluster can thus be modeled, after *perfectly* canceling $m - 1$ strong interferences, as follows:

$$I_{\text{intra}}^m = \sum_{j=m+1}^{\bar{c}} S_{(j)} \approx \sum_{\substack{j=m+1 \\ y_j \in \mathcal{N}^{x_0}}}^{\bar{c}} P_u h_{y_j x_0} \|y_{(j)}\|^{-\alpha}, \quad (6)$$

where $\|y_{(j)}\| = r_{(j)}$. Note that the ranking is applied only at the distances $\|y_{(j)}\|^{-\alpha}$ as per the approximation. The SINR experienced by any user at m^{th} rank in the representative cluster can therefore be defined as follows:

$$\text{SINR}_m = \frac{S_{(m)}}{I_{\text{agg}}^m} = \frac{S_{(m)}}{I_{\text{intra}}^m + I_{\text{inter}} + N_0}. \quad (7)$$

2) *Imperfect SIC and Detection Probability*: The signals from $m-1$ interferers (who are located closer to the BS than the rank m user) may or may not be decoded perfectly; therefore, SIC may or may not be performed in a perfect fashion. In such a case, we first define the probabilities for the successful detection of the signals of the ranked users (ranked in terms of their distances), respectively, as follows:

$$\begin{aligned} p_{(1)} &= \mathbb{P} \left(\frac{S_{(1)}}{I_{\text{agg}}^1} \geq \theta \right), \\ p_{(2)} &= p_{(1)} \mathbb{P} \left(\frac{S_{(2)}}{I_{\text{agg}}^2} \geq \theta \right) + \bar{p}_{(1)} \mathbb{P} \left(\frac{S_{(2)}}{I_{\text{agg}}^2 + S_{(1)}} \geq \theta \right), \\ p_{(3)} &= p_{(1)} p_{(2)} \mathbb{P} \left(\frac{S_{(3)}}{I_{\text{agg}}^3} \geq \theta \right) + \bar{p}_{(1)} p_{(2)} \mathbb{P} \left(\frac{S_{(3)}}{I_{\text{agg}}^3 + S_{(1)}} \geq \theta \right) \\ &\quad + \bar{p}_{(2)} p_{(1)} \mathbb{P} \left(\frac{S_{(3)}}{I_{\text{agg}}^3 + S_{(2)}} \geq \theta \right) + \bar{p}_{(1)} \bar{p}_{(2)} \mathbb{P} \left(\frac{S_{(3)}}{I_{\text{agg}}^3 + \sum_{j=1}^2 S_{(j)}} \geq \theta \right), \end{aligned}$$

where $p_{(j)}$ and $\bar{p}_{(j)}$, $\forall j = 1, 2, 3, \dots$, represent the probability of successful and unsuccessful detection of j -th ranked user's signal, respectively. It can be seen that the BS attempts to decode the closest user without any interference cancellation. If the decoding is unsuccessful, the interference from this user remains intact. Subsequently, we can generalize the detection probability of a user at m -th rank as follows:

$$p_{(m)} = \sum_{\mathbf{b} \in \mathcal{B}} A \mathbb{P} \left(\frac{S_{(m)}}{I_{\text{agg}}^m + \sum_{j=1}^{m-1} (1 - b(j)) S_{(j)}} \geq \theta \right), \quad (8)$$

where $A = \left(\prod_{j=1}^{m-1} (p_{(j)})^{b(j)} (\bar{p}_{(j)})^{1-b(j)} \right)$, θ is the signal detection threshold, and \mathcal{B} denotes the set of 2^{m-1} combinations in which each combination \mathbf{b} has $m-1$ bits. The successful detection is represented by a binary digit $b(j) = 1$ whereas the detection failure is given by $b(j) = 0$. The intra-cluster interference experienced by a user at rank m thus depends on whether the detections for $m-1$ closer users were successful or not. As such, conditioned on a given combination \mathbf{b} , the SINR experienced by a user at rank m can be modeled as:

$$\text{SINR}_{m,\mathbf{b}} = \frac{S_{(m)}}{I_{\text{intra}}^{m,\mathbf{b}} + I_{\text{inter}} + N_0}, \quad (9)$$

where

$$I_{\text{intra}}^{m,\mathbf{b}} = I_{\text{intra}}^m + I_{\text{add}}^m = I_{\text{intra}}^m + \sum_{j=1}^{m-1} (1 - b(j)) S_{(j)}.$$

Note that, even after successful detection, a given user can still experience rate outage (i.e., the achievable rate may remain below the target rate requirement).

C. Performance Metrics

We analyze the performance gains of uplink NOMA considering a system where each user has a target data rate requirement. For this case, the rate coverage probability of a user at rank m and the mean rate coverage probability of a cluster are relevant performance metrics. These metrics are defined for different SIC scenarios in the following.

1) *Rate Coverage*: Rate coverage probability is the probability that a given user's achievable rate remains above the target data rate. Mathematically, the rate coverage probability of a user at m -th rank can be defined as $\mathbb{P}(\log_2(1 + \text{SINR}_m) \geq R_m)$, where R_m is the target data rate requirement of the m -th ranked user. Now, we define the rate coverage probability of m -th user in the following specific cases:

- *Rate Coverage with Perfect SIC*: Using the definition of SINR_m from (7), the rate coverage probability of a user at rank m in the representative cluster can be defined as:

$$\mathcal{C}_m^{(P)} = \mathbb{P}(\text{SINR}_m \geq \gamma_m) = \mathbb{P}\left(\frac{S_{(m)}}{I_{\text{agg}}^m} \geq \gamma_m\right), \quad (10)$$

where $\gamma_m = 2^{R_m} - 1$ is the desired SINR corresponding to the rate requirement R_m of the user at rank m .

- *Rate Coverage with Imperfect SIC*: In this case, we consider the probability of decoding/canceling interferences from $m - 1$ closer interferers as less than one. As such, the rate coverage probability of a user at rank m needs to consider all possible combinations $\mathbf{b} \in \mathcal{B}$ and thus can be defined using (9) as follows:

$$\mathcal{C}_m^{(I)} = \sum_{\mathbf{b} \in \mathcal{B}} A\mathbb{P}(\text{SINR}_{m,\mathbf{b}} \geq \gamma_m). \quad (11)$$

- *Rate Coverage with Imperfect SIC - Worst Case*: The worst-case model assumes that the decoding of any user at rank m is always unsuccessful whenever the decoding of his relative $m - 1$ closer users is unsuccessful. Such a worst-case model is simple and allows evaluating the impact of SIC error propagation on the NOMA performance without invoking complicated NOMA specific link-to-system mapping. The worst-case detection probability of a user at rank m can therefore be given as:

$$p_{(m)}^{\text{worst}} = \prod_{i=1}^{m-1} \mathbb{P}(\text{SINR}_i \geq \theta), \quad (12)$$

where SINR_i can be given using (7). The rate coverage probability of a user at rank m can thus be given as:

$$\mathcal{C}_m^{\text{worst}} = p_{(m)}^{\text{worst}} \mathcal{C}_m^{(P)}. \quad (13)$$

As a by-product, we can evaluate the rate coverage of a user at rank m in an equivalent TDMA-based OMA system where \bar{c} users in a cluster are served in orthogonal time slots. The rate of a user at rank m in OMA system can be defined as $R_m^{(\text{oma})} = \frac{1}{\bar{c}} \log_2(1 + \text{SINR}_m^{\text{oma}})$. For fair comparison with NOMA, we need to include the scaling factor of $\frac{1}{\bar{c}}$ which shows the portion of available resources to a given user in OMA system. As such, if the target rate requirement of the user is R_{th} , the desired SINR threshold $\gamma_m^{(\text{oma})}$ can be defined as $2^{R_{\text{th}}\bar{c}} - 1$. Subsequently, substituting zero intra-cluster interference, $\bar{c} = 1$ for inter-cell interfering clusters, and replacing $\gamma_m = \gamma_m^{(\text{oma})}$ in the rate coverage expressions of NOMA, we can determine the rate coverage of a user at rank m in an OMA system.

Further, we can also calculate the average rate of a user at rank m . For perfect SIC, imperfect SIC, and worst case SIC scenarios, average rates for a user at rank m can be computed, respectively, as follows:

$$\begin{aligned}\mathcal{R}_m^{(\text{P})} &= \mathbb{E}[\ln(1 + \text{SINR}_m)] = \int_0^\infty \mathbb{P}(\text{SINR}_m > e^t - 1) dt, \\ \mathcal{R}_m^{(\text{I})} &= \sum_{b \in \mathcal{B}} A \int_0^\infty \mathbb{P}(\text{SINR}_{m,b} > e^t - 1) dt, \\ \mathcal{R}_m^{\text{worst}} &= p_{(m)}^{\text{worst}} \mathcal{R}_m^{(\text{P})}.\end{aligned}$$

Substituting $e^t - 1$ in place of γ_m , we can integrate all coverage probability expressions over t to evaluate the average rate of a user at rank m numerically. In addition, substituting $m = 1$ and $m = \bar{c}$, we can characterize the performance of the closest and farthest user in a NOMA cluster, respectively.

2) *Mean Rate Coverage of a Cluster:* Although the individual rate coverage of a user in the representative cluster is a useful metric, it does not offer a complete insight related to the cumulative performance of the users in the representative NOMA cluster. As such, we consider analyzing the collective performance of all users by defining the mean rate coverage of all users in the representative NOMA cluster as follows:

$$\mathcal{O} = \sum_{m=1}^{\bar{c}} \frac{\mathcal{C}_m^{(\cdot)}}{\bar{c}}, \quad (14)$$

where $(\cdot) = \text{P, I, and worst}$ for perfect SIC, imperfect SIC, and worst case SIC, respectively.

IV. RELEVANT DISTANCE DISTRIBUTIONS FOR THE CHARACTERIZATION OF INTERFERENCE

In this section, we characterize the relevant distributions of the distances between the BS of a representative cluster and different intra-cell user devices that are ordered according to their distances. These distance distributions are crucial for deriving the Laplace transforms of the intra-cluster interferences and the rate coverage analysis.

As mentioned in the Approximation, we consider ranking the users in terms of their distances from the serving BS, which is located at the cluster center. Consequently, we characterize the distance distributions

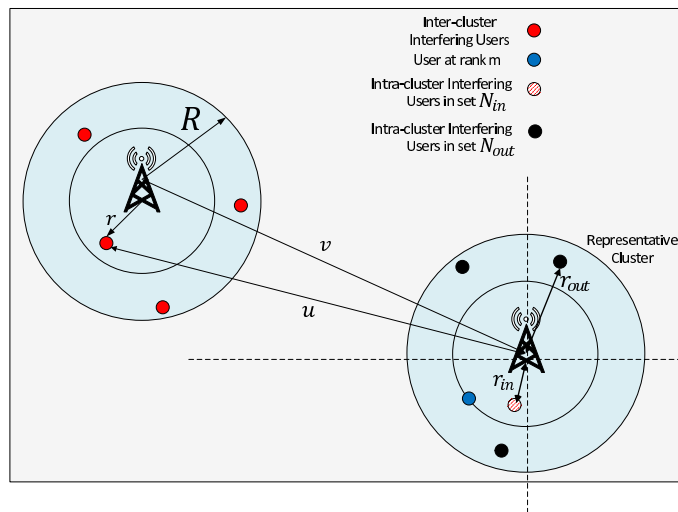


Fig. 2: Illustration of the representative cluster, intra-cluster, and inter-cluster interferers along with their relevant distances.

of the m^{th} closest node as well as its respective intra-cluster interfering nodes from the BS. Note that the distance of any arbitrary intra-cluster device located at $y \in \mathbb{R}^2$ with respect to $x_0 \in \mathbb{R}^2$ is i.i.d. and follows the uniform distribution given in (1). Subsequently, the distance $\|y\| = r$ of any arbitrary intra-cluster device from the representative BS follows a sampling distribution given by $f_r(r)$ in (2). Now we order \bar{c} devices within the representative cluster with respect to the cluster center such that $r_{(1)} \leq r_{(2)} \leq \dots \leq r_{(\bar{c})}$. The distance distribution of the user at rank m can thus be given as follows.

Lemma 1 (Distribution of the Distance of the User at rank m). *For a Matern cluster process, the distribution of the distance of a user at rank m in the representative cluster, i.e., $r_{(m)}$ from its serving BS follows a Generalized Beta (GB) distribution of the first kind. The distance distribution can be derived as:*

$$f_{r_{(m)}}(r) = \text{GB}(r, 2, R, m, \bar{c} - m + 1) = \frac{2r^{2m-1} \left(1 - \frac{r^2}{R^2}\right)^{\bar{c}-m}}{R^{2m} B(m, \bar{c} - m + 1)},$$

where $B(\cdot)$ denotes the Euler Beta function. GB distribution includes Beta distribution, Generalized Gamma distribution, and Pareto distribution as its special cases.

Proof: See **Appendix A**. ■

Provided that the user of interest is at rank m , we now characterize the distribution of the distances of its corresponding intra-cluster interfering devices. Note that the possible interfering nodes for a user at rank m can lie at any place (depending on the perfect and imperfect SIC) except the location of the user at rank m . As such, the set of intra-cluster interferers can be partitioned into two subsets, i.e., $\mathcal{N}_{\text{in}}^{x_0} \in \{1, 2, \dots, m-1\}$ and $\mathcal{N}_{\text{out}}^{x_0} \in \{m+1, \dots, \bar{c}\}$ where $\mathcal{N}_{\text{in}}^{x_0}$ and $\mathcal{N}_{\text{out}}^{x_0}$ represent the set of interfering

nodes closer and farther to the reference BS, respectively, compared to the user at rank m . This set-up is demonstrated in Fig. 2. Consequently, the distances from the representative BS to devices in $\mathcal{N}_{\text{in}}^{x_0}$ are i.i.d as shown by *Afshang et al.* in [13], [14], [23], [24]. The same property holds for the users in $\mathcal{N}_{\text{out}}^{x_0}$.

Lemma 2 (Conditional Distribution of the Distances of Intra-Cluster Interfering Users). *Conditioned on the distance of the user of interest at rank m (say $r_{(m)} = \hat{r}$), the distribution of the distance r_{in} of any device in the set $\mathcal{N}_{\text{in}}^{x_0} \in \{1, 2, \dots, m-1\}$ from cluster center (BS) is i.i.d and can therefore be given by:*

$$f_{r_{\text{in}}}(r_{\text{in}}|\hat{r}) = \frac{f_r(r_{\text{in}})}{F_r(\hat{r})} = \frac{2r_{\text{in}}}{\hat{r}^2}, \quad r_{\text{in}} < \hat{r}. \quad (15)$$

Similarly, the distribution of the distance of any device in the set $\mathcal{N}_{\text{out}}^{x_0} \in \{m+1, \dots, \bar{c}\}$ from cluster center (BS) is conditionally i.i.d. and can be given as:

$$f_{r_{\text{out}}}(r_{\text{out}}|\hat{r}) = \frac{f_r(r_{\text{out}})}{1 - F_r(\hat{r})} = \frac{2r_{\text{out}}}{R^2 - \hat{r}^2}, \quad R \geq r_{\text{out}} > \hat{r}, \quad (16)$$

where r_{in} and r_{out} are conditionally independent.

Proof: The proof can be done along the same lines as shown in [13]. For sake of completeness of the paper, we discuss it briefly in **Appendix B**. ■

At this point, it is noteworthy that **Lemma 2** utilizes the fact that the ordering of users in the set $\mathcal{N}_{\text{out}}^{x_0}$ does not have any impact on the cumulative interference generated from all users of this set. Therefore, the interfering devices in the set $\mathcal{N}_{\text{out}}^{x_0}$ can be sampled randomly without any specific ordering. Consequently, the distance distributions of the interfering users belonging to set $\mathcal{N}_{\text{out}}^{x_0}$ are i.i.d. and can be given as in **Lemma 2**. The same statements hold for the users in set $\mathcal{N}_{\text{in}}^{x_0}$.

Nonetheless, for imperfect SIC scenarios, we need to include specific interferences from the ranked users in set $\mathcal{N}_{\text{in}}^{x_0}$ whose signals go undetected. As such, for each combination \mathbf{b} , we need to include additional intra-cluster interferences from the specific users whose corresponding $b(i) = 1$ in set $\mathcal{N}_{\text{in}}^{x_0}$. Given that the user of interest is at rank m , the distance distribution of a user at specific rank $j < m$, can be derived by exploiting the conditional ranked distributions from the theory of order statistics as in the following.

Lemma 3 (Conditional Distribution of the Distance of an Intra-Cluster Interfering User at Rank j). *Given that the user of interest is at rank m (say $r_{(m)} = \hat{r}$), the conditional distribution of the distance of j -th rank user, such that $j > m$ and $r_{(j)} > r_{(m)} = \hat{r}$, is the distribution of the $j - m$ -th order statistics of $\bar{c} - m$ i.i.d. distance variables whose PDF is the truncated PDF of r as given in (16). The conditional*

distance distribution of j -th rank user can thus be given as:

$$f_{r_{(j)}|r_{(m)}=\hat{r}}(\gamma_j) = \frac{2\gamma_j(\bar{c}-m)!(\gamma_j^2 - \hat{r}^2)^{j-m-1}(R^2 - \gamma_j^2)^{\bar{c}-j}}{\Gamma(j-m)(\bar{c}-j)!(R^2 - \hat{r}^2)^{\bar{c}-m}}. \quad (17)$$

Accordingly, the conditional distribution of the distance of j -th rank user, such that $j < m$ and $r_{(j)} < r_{(m)} = \hat{r}$, is the same as the distribution of the j -th order statistics of $m-1$ i.i.d. distance variables whose PDF is the truncated PDF of r as given in (15). The conditional distance distribution of j -th rank user can thus be given as:

$$f_{r_{(j)}|r_{(m)}=\hat{r}}(\gamma_j) = \frac{2\Gamma(m)(\hat{r}^2 - \gamma_j^2)^{m-j-1}(\gamma_j)^{2j-1}}{\Gamma(m-j)\Gamma(j)\hat{r}^{2m-2}}. \quad (18)$$

Proof: The proof of the first part of the lemma follows by substituting the PDF from (16) and its corresponding CDF into (A.1) and replacing \bar{c} with $\bar{c} - m$ and m with $j - m$. Similarly, the proof of the second part of the lemma follows by substituting the PDF from (15) and its corresponding CDF into (A.1) and replacing \bar{c} with $m - 1$ and m with j . ■

V. RATE COVERAGE ANALYSIS

Using the distance distributions derived in Section IV, in this section, we derive the Laplace transforms of the intra-cluster interferences experienced by the transmission of m -th rank user considering both the perfect and imperfect SIC scenarios. We then derive the Laplace transform of the inter-cluster interference incurred at the representative BS by exploiting the distance distributions from geometric probability and a less complex upper bound of the Laplace Transform of the inter-cluster interference. Finally, we derive the rate coverage expressions for NOMA as well as OMA system.

A. Laplace Transforms of the Intra-Cluster Interferences

As defined in (6), it is evident that the intra-cluster interference with perfect SIC is due to all users that are located beyond the distance $\hat{r} = r_{(m)}$. Subsequently, the intra-cluster interference defined in (6) can be rewritten as follows:

$$I_{\text{intra}}^m = \sum_{y \in \mathcal{N}_{\text{out}}^{x_0}} P_u h_{y_{x_0}} \|y\|^{-\alpha}. \quad (19)$$

The Laplace transform of I_{intra}^m can then be given as follows.

Lemma 4 (Laplace transform of the Intra-Cluster Interference with Perfect SIC). *The intra-cluster interference experienced by the transmission of m -th ranked user in the cluster, with perfect SIC, can be given as follows:*

$$\mathcal{L}_{I_{\text{intra}}^m}(s) = \left(\frac{2s^{\frac{2}{\alpha}} \tilde{\mathbf{B}}[-\frac{R^\alpha}{s}, -\frac{\hat{r}^\alpha}{s}, \frac{2+\alpha}{\alpha}, 0]}{(R^2 - \hat{r}^2)(-1)^{\frac{2}{\alpha}} \alpha} \right)^{\bar{c}-m}, \quad (20)$$

where $\tilde{\mathbf{B}}(\cdot)$ is the generalized incomplete Beta function.

Proof: See **Appendix C**. ■

For cases of practical interest such as $\alpha = 4$, the result presented in the Lemma 4 can be further simplified as follows.

Corollary 1 (Laplace transform of the Intra-Cluster Interference with Perfect SIC, $\alpha = 4$). *When $\alpha = 4$, the Laplace transform of the intra-cluster interference experienced by the transmission of m -th ranked user in the cluster, with perfect SIC, can be further simplified as follows.*

$$\begin{aligned} \mathcal{L}_{I_{\text{intra}}^m}(s) &= \left(1 - \frac{\sqrt{P_u s} \left(\tan^{-1}\left(\frac{\hat{r}^2}{\sqrt{P_u s}}\right) - \tan^{-1}\left(\frac{R^2}{\sqrt{P_u s}}\right) \right)}{\hat{r}^2 - R^2} \right)^{\bar{c}-m}, \\ &\stackrel{(a)}{=} \left(1 - \frac{\sqrt{P_u s} \tan^{-1}\left(\frac{\sqrt{P_u s}(\hat{r}^2 - R^2)}{P_u s + \hat{r}^2 R^2}\right)}{\hat{r}^2 - R^2} \right)^{\bar{c}-m}, \end{aligned}$$

where (a) is derived by using the property $\tan^{-1}(x) - \tan^{-1}(y) = \tan^{-1}\left(\frac{x-y}{1+xy}\right)$. Note that, if $m = \bar{c}$, which represents the farthest user from the BS, there is no intra-cluster interference since $\bar{c} - m = 0$.

Further, an accurate second-order approximation of $\tan^{-1}(x)$ with a maximum absolute error of 0.0053 rad can be derived as $\tan^{-1}(x) \approx \frac{\pi}{4}x + 0.273x|1-x|$. With this approximation, the closed-form expression presented in Corollary 1 can be further simplified.

The intra-cluster interference incurred at a BS with imperfect SIC is defined in (9). It can be seen that the intra-cluster interference is composed of two parts, i.e., the interference observed from all users in set $\mathcal{N}_{\text{out}}^{x_0}$ that are located beyond the distance $\hat{r} = r_{(m)}$ and the interference from users in set $\mathcal{N}_{\text{in}}^{x_0}$ whose signals go undetected. The Laplace transform of the intra-cluster interference with imperfect SIC can then be derived in closed-form as follows.

Lemma 5 (Laplace transform of the Intra-Cluster Interference with ImPerfect SIC). *The intra-cluster interference experienced by the transmission of m -th ranked user in the cluster, with imperfect SIC, can be given as follows:*

$$\mathcal{L}_{I_{\text{intra}}^{m,b}}(s) \stackrel{(a)}{=} \mathcal{L}_{I_{\text{intra}}^m}(s) \mathcal{L}_{I_{\text{add}}^m}(s),$$

where (a) follows from the fact that, conditioned on the serving distance of m -th user, $\mathcal{N}_{\text{in}}^{x_0}$ and $\mathcal{N}_{\text{out}}^{x_0}$ are independent and the interfering distance distributions of their respective users are also independent. Note that $\mathcal{L}_{I_{\text{intra}}^m}(s)$ is given in Lemma 4 and $\mathcal{L}_{I_{\text{add}}^m}(s)$ can be derived as follows:

$$\mathcal{L}_{I_{\text{add}}^m}(s) = \prod_{j=1}^{m-1} \left(\sum_{i=0}^{m-j-1} K(i) \frac{s^{\frac{2+2i}{\alpha}} \mathbf{B}\left[\frac{-\hat{r}^\alpha}{s}, 1 + \frac{2+2i}{\alpha}, 0\right]}{\hat{r}^{2(j+i)}} \right)^{1-b(j)},$$

where $K(i) = \frac{2\Gamma[m](-1)^{i-\frac{2+2i}{\alpha}-1}}{\Gamma[j]\Gamma[i+1]\Gamma[m-j-i]\alpha}$ and $\mathbf{B}(\cdot)$ is the incomplete Beta function.

Proof: See **Appendix D**. ■

B. Laplace transforms of the Inter-Cluster Interference

Typically, the Laplace transform of the inter-cluster interference in PCP is characterized for a fixed-distance typical link (where the receiver is not chosen from the PCP) [12]. Recently, a more general approach is presented in [13], [14] to characterize the inter-cluster interference in which both the transmitter and receiver can be chosen from the PCP. Also, it was shown in [13], [14] that both the intra/inter-cluster interfering distances can be modeled using Rice distributions for Modified Thomas Cluster Processes.

Given the definition of the inter-cluster interference in (5), $I_{\text{inter}} = \sum_{x \in \Phi_m \setminus x_0} \sum_{y \in \mathcal{N}^x} P_u h_{yx} \|x + y\|^{-\alpha}$ and following a similar approach proposed in [13], we can write the Laplace transform $\mathcal{L}_{\text{inter}}(s)$ as follows:

$$\begin{aligned} \mathcal{L}_{\text{inter}}(s) &\stackrel{(a)}{=} \mathbb{E} \left[e^{-s \sum_{x \in \Phi_m \setminus x_0} \sum_{y \in \mathcal{N}^x} P_u h_{yx} \|x + y\|^{-\alpha}} \right], \\ &\stackrel{(b)}{=} \mathbb{E} \left[\prod_{x \in \Phi_m \setminus x_0} \prod_{y \in \mathcal{N}^x} \mathbb{E}_h [e^{-P_u h_{yx} \|x + y\|^{-\alpha}}] \right], \\ &\stackrel{(c)}{=} \mathbb{E} \left[\prod_{x \in \Phi_m \setminus x_0} \left(\mathbb{E}_y \left[\frac{1}{1 + s P_u \|x + y\|^{-\alpha}} \right] \right)^{\bar{c}} \right], \\ &\stackrel{(d)}{=} \exp \left[-\lambda_m \int_{\mathbb{R}^2} \left(1 - \left(\int_{\mathbb{R}^2} \frac{1}{1 + s P_u \|x + y\|^{-\alpha}} f_Y(y) dy \right)^{\bar{c}} \right) dx \right], \\ &\stackrel{(e)}{=} \exp \left[-2\pi \lambda_m \int_0^\infty \left(1 - \left(\int_u \frac{1}{1 + s P_u u^{-\alpha}} f_U(u|v) du \right)^{\bar{c}} \right) v dv \right], \end{aligned}$$

where (a) follows from the definition of the Laplace transform and (b) follows from the property of the exponential function. Conditioned on the distance $v = \|x\|$ from the representative BS to the cluster center $x \in \Phi_m$, the distance of each user device within the cluster (whose center is located at x) to the representative BS is i.i.d. Subsequently, (c) follows from the fact that the distances of all users in an interfering cluster to the reference BS are i.i.d., (d) follows from the PGFL of PPP since all cluster centers x follow a homogeneous PPP, and (e) follows from the conversion of Cartesian to polar coordinates. The Laplace transform can thus be derived as follows.

Lemma 6 (Laplace Transform of the Inter-Cluster Interference). *Given the distance v as illustrated in Fig. 2, the conditional distribution of u can be given for the cases (i) $v \geq R$ and (ii) $v < R$, respectively, as follows [25], [26]:*

$$f_{U|v \geq R}(u) = \frac{u^2}{R^2} - \frac{2u^2}{R^2} \sin^{-1} \left(\frac{v^2 - R^2 + u^2}{2uv} \right), \quad (21)$$

where $v - R \leq u \leq R + v$. For the case $v < R$, we have:

$$f_{U|v < R}(u) = \begin{cases} \frac{2u}{R^2}, & 0 \leq u \leq R - v, \\ \frac{u^2}{R^2} - \frac{2u^2}{R^2} \sin^{-1} \left(\frac{v^2 - R^2 + u^2}{2uv} \right), & R - v \leq u \leq R + v. \end{cases} \quad (22)$$

Subsequently, $\mathcal{L}_{\text{inter}}(s)$ can be defined using (21) and (22) as:

$$\mathcal{L}_{\text{inter}}(s) = \exp(-2\pi\lambda_m (\mathcal{A}_1 + \mathcal{A}_2)), \quad (23)$$

where

$$\mathcal{A}_1 = \int_0^R \left(1 - \underbrace{\left(\int_u \frac{1}{1 + sP_u u^{-\alpha}} f_{U|v < R}(u) du \right)}_{I_1} \right)^{\bar{c}} v dv,$$

$$\mathcal{A}_2 = \int_R^\infty \left(1 - \underbrace{\left(\int_u \frac{1}{1 + sP_u u^{-\alpha}} f_{U|v \geq R}(u) du \right)}_{I_2} \right)^{\bar{c}} v dv.$$

The integrals I_1 and I_2 are solvable in closed-form as detailed in **Appendix E** and the Laplace transform as well as the rate coverage can be evaluated numerically using MAPLE and MATHEMATICA.

Note that the Laplace transform in (d) can also be attained from the PGFL of an MCP with fixed number of daughters per cluster as defined below.

Definition 3 (PGFL of the Matern Cluster Process). *The PGFL of the MCP given the number of nodes are fixed \bar{c} per cluster can be given as follows:*

$$\mathbb{E} \left[\prod_{x \in \Phi_m} v(x) \right] = \exp \left[-\lambda \int_{\mathbb{R}^2} (1 - Z(v(x))^{\bar{c}}) dx \right], \quad (24)$$

where λ denotes the intensity of the parent point process which is a homogeneous PPP in case of MCP and $Z(v(x)) = \int_{\mathbb{R}^2} v(x+y) f(y) dy = \mathbb{E}_y[v(x+y)]$. Since the original cluster process is stationary, the inter-cluster interference is independent of the position of the receiver [12].

Now observing that $Z(v(x))^{\bar{c}} = \mathbb{E}_y[v(x+y)]^{\bar{c}} = \mathbb{E}_y \left[\frac{1}{(1 + sP_u ||x+y||^{-\alpha})^{\bar{c}}} \right]^{\bar{c}}$, we can apply Jensen inequality $\mathbb{E}_y[a]^{\bar{c}} \leq \mathbb{E}_y[a^{\bar{c}}]$ to derive an upper bound on the Laplace transform of the inter-cluster interference. That is

$$\mathcal{L}_{\text{inter}}(s) \stackrel{(a)}{\leq} \int_{\mathbb{R}^2} \left(1 - \mathbb{E}_y \left[\frac{1}{(1 + sP_u ||x+y||^{-\alpha})^{\bar{c}}} \right] \right) dx, \quad (25)$$

$$= \int_{\mathbb{R}^2} \int_{\mathbb{R}^2} \left(1 - \frac{1}{(1 + sP_u ||x+y||^{-\alpha})^{\bar{c}}} \right) f_Y(y) dy dx, \quad (26)$$

$$\stackrel{(b)}{=} \exp\left(-\pi\lambda_m(sP_u)^{\frac{2}{\alpha}}\bar{c}B\left[1 - \frac{2}{\alpha}, \bar{c} + \frac{2}{\alpha}\right]\right), \quad (27)$$

where (a) follows from applying the Jensen inequality and (b) follows from applying the cartesian-to-polar coordinate transformation and integration by parts [15].

C. Rate Coverage Probability for NOMA

In this section, we derive the rate coverage probability of a user at rank m for all three cases, i.e., perfect SIC, imperfect SIC, and worst-case SIC.

1) *Rate Coverage with Perfect SIC*: Using the distance distribution of the user at rank m derived in **Lemma 1** and the Laplace transforms of the inter- and intra-cluster interferences derived, respectively, in **Lemma 4** and **Lemma 6**, the SINR coverage of a user at rank m can be derived as follows:

$$\begin{aligned} \mathcal{C}_m^{(P)} &= \mathbb{P}\left(\frac{P_u h_{y_{x_0}} \hat{r}^{-\alpha}}{I_{\text{agg}}^m + N_0} \geq \gamma_m\right) = \exp\left(-\frac{\gamma_m(I_{\text{agg}}^m + N_0)}{P_u \hat{r}^{-\alpha}}\right), \\ &\stackrel{(a)}{=} \int_0^R e^{-\frac{\gamma_m N_0}{P_u \hat{r}^{-\alpha}}} \mathcal{L}_{I_{\text{intra}}^m}\left(\frac{\gamma_m}{P_u \hat{r}^{-\alpha}}\right) \mathcal{L}_{I_{\text{inter}}}\left(\frac{\gamma_m}{P_u \hat{r}^{-\alpha}}\right) f_{\hat{r}}(\hat{r}) d\hat{r}, \end{aligned} \quad (28)$$

where (a) follows from averaging over the distribution of \hat{r} and the definition $I_{\text{agg}}^m = I_{\text{inter}} + I_{\text{intra}}^m$. Since NOMA systems are typically interference limited, the expression in (a) can be further simplified by substituting $N_0 = 0$. Also, taking $\alpha = 4$ and taking the upper bound of the Laplace transform of the inter-cluster interference in (25), we can simplify (28) as follows:

$$\sum_{i=0}^{c-m} \int_0^1 \frac{G(i) (1 - \sqrt{\gamma_m} z \cot^{-1}(\sqrt{\gamma_m} z))^i}{e^{zR^2 \sqrt{\gamma_m} \bar{c} \lambda_m B[1/2, 1/2 + \bar{c}]} z^{i+1-\bar{c}}} dz,$$

where

$$G(i) = \frac{(\sqrt{\gamma_m} \cot^{-1} \sqrt{\gamma_m} - 1)^{\bar{c}-m-i} \binom{\bar{c}-m}{i}}{B[m, 1 + \bar{c} - m]}.$$

2) *Rate Coverage with Imperfect SIC*: In this case, a given user at rank m is prone to the interferences from all users in the set $\mathcal{N}_{\text{out}}^{x_0}$ as well as from some users in the set $\mathcal{N}_{\text{in}}^{x_0}$ whose signals go undetected. As such, using the distance distribution of the user at rank m derived in **Lemma 1**, the Laplace transforms of the intra- and inter-cluster interferences derived, respectively, in **Lemma 5** and **Lemma 6**, and the interference limited case, the SIR coverage of a user at rank m in the representative cluster can be derived as follows:

$$\mathcal{C}_m^{(I)} = \int_0^R \mathcal{L}_{I_{\text{intra}}^{m,b}}\left(\frac{\eta_m}{P_u \hat{r}^{-\alpha}}\right) \mathcal{L}_{I_{\text{inter}}}\left(\frac{\eta_m}{P_u \hat{r}^{-\alpha}}\right) f_{\hat{r}}(\hat{r}) d\hat{r}. \quad (29)$$

3) *Rate Coverage with Imperfect SIC-Worst Case*: The rate coverage probability with the worst case mapping can be derived as $\mathcal{C}_m^{\text{worst}} = p_{(m)}^{\text{worst}} \mathcal{C}_m^{(P)}$, where $\mathcal{C}_m^{(P)}$ is given using (28). Note that the derivation of

the detection probability $p_{(m)}^{\text{worst}}$ defined in (12) can be done by replacing γ_m with θ in (28) for each user at j -th rank.

D. Rate Coverage Probability for OMA

The rate coverage performance of a user at rank m in a given OMA cluster can be derived as follows.

Corollary 2 (Rate Coverage Probability of a User at Rank m in OMA). *The rate coverage probability of a user at rank m in TDMA-based OMA system can be given by taking zero intra-cluster interference, using the Laplace transform of the inter-cluster interference from (23) with $\bar{c}=1$, and replacing γ_m with $\gamma_m^{(\text{oma})}$ as follows:*

$$\mathcal{C}_m^{(\text{oma})} \stackrel{(a)}{=} \int_0^R e^{-\frac{\gamma_m^{(\text{oma})} N_0}{P_u \hat{r}^{-\alpha}}} \mathcal{L}_{I_{\text{inter}}}^{(\text{oma})} \left(\frac{\gamma_m^{(\text{oma})}}{P_u \hat{r}^{-\alpha}} \right) f_{\hat{r}}(\hat{r}) d\hat{r}, \quad (30)$$

$$\stackrel{(b)}{=} \gamma[\bar{c} + 1] {}_1\tilde{F}_1[m, 1 + \bar{c}, -KR^2], \quad (31)$$

where $K = (\gamma_m^{(\text{oma})})^{2/\alpha} \bar{c} \lambda_m B[1 - 2/\alpha, 2/\alpha + \bar{c}]$ and ${}_1\tilde{F}_1[\cdot]$ is the regularized confluent Hypergeometric function.

Note that (b) is derived by neglecting the noise, taking the bound of the inter-cluster interference in (25), and solving the integral in (a) in closed-form.

VI. NUMERICAL RESULTS

In this section, we investigate the performance of NOMA and OMA in clustered cellular networks. We conduct a comparative analysis with the conventional PPP-based cellular network model to demonstrate that how two different modeling approaches may impact the accuracy of the conclusions related to the performance of NOMA versus OMA. The accuracy of the derived rate coverage expressions is validated by comparing them in the results with the Monte-Carlo simulations. The performance of the uplink NOMA versus uplink OMA system is investigated as a function of the maximum coverage radius of clusters, users per cluster, intensity of the BSs, and the target rate requirements per user.

The locations of users are drawn from a Poisson cluster process in a square region with area $|A| = 10 \times 10 \text{ km}^2$. The cluster centers are spatially distributed as a PPP with intensity λ_m and the users are scattered uniformly around them. We set the threshold for successful demodulation and decoding as 0 dB. The number of users per cluster is taken as $\bar{c} = 8$ and the radius of each cluster is set to $r = 0.8 \text{ km}$. We set the path-loss exponent to $\beta = 4$ and the thermal noise power density to $\sigma^2 = 1 \times 10^{-14} \text{ W/Hz}$. The transmit powers of users are taken as $P_u = 2 \text{ W}$. The target rate requirement of each user is taken as $R_{\text{th}} = 3 \text{ bps/Hz}$. The values of the aforementioned parameters remain the same unless stated otherwise.

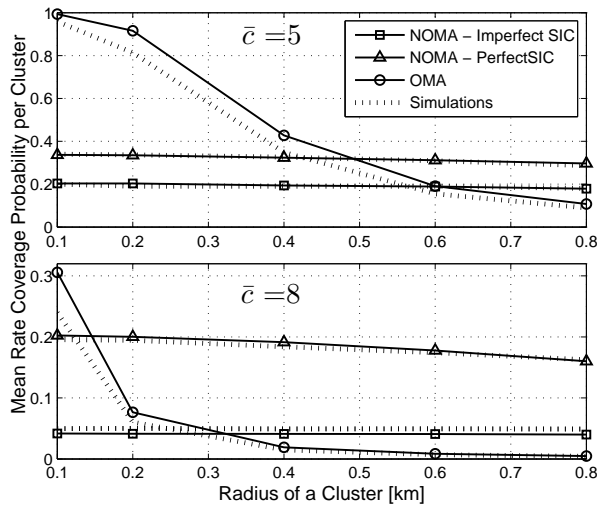


Fig. 3: Mean rate coverage probability as a function of the radius of each cluster in the single-tier cellular network, $\lambda_m|A| = 2$.

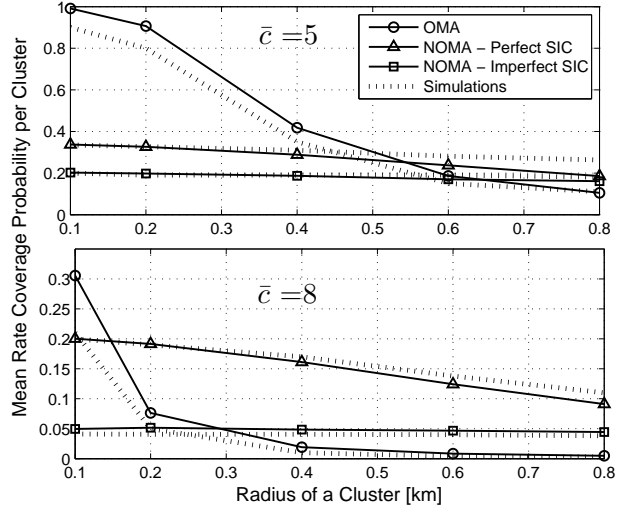


Fig. 4: Mean rate coverage probability as a function of the radius of each cluster in the single-tier cellular network, $\lambda_m|A| = 8$.

A. Impact of the Coverage Radius of a BS

Fig. 3 depicts the average rate coverage of \bar{c} users in a NOMA representative cluster as a function of the maximum cell/cluster radius R with $\lambda_m|A| = 2$. This scenario can be considered as intra-cell interference-limited due to low intensity of BSs. The results are compared with the mean rate coverage of \bar{c} users in an equivalent OMA system where one user transmits at a time in each cell/cluster.

First, it can be seen that the average rate coverage of the OMA cluster is higher than the NOMA cluster for small values of R . The reason is no intra-cell interference in the OMA system and higher intra-cell interference in the NOMA system due to the vicinity of users and the representative BS. Nonetheless, as R increases, the performance of OMA reduces significantly due to notable path-loss degradation of weak users. However, interestingly, the performance of NOMA system remains nearly the same since the effect of path-loss degradation gets nearly cancelled by the reduction of intra-cell interference. As a result, beyond a certain coverage radius of a BS, the gains of NOMA become evident.

Further, we note that the performances of OMA and NOMA depend significantly on the number of users per cluster \bar{c} . As \bar{c} increases, the mean coverage probability reduces for both the OMA and NOMA systems. In OMA, the reduction is caused due to further splitting of resources, whereas in NOMA the reduction is caused due to the increased intra-cell interference. We also note that the rate coverage decay with \bar{c} is more severe for OMA since the rate is a direct function of the amount of consumed resources. Due to this reason, NOMA starts to outperform OMA for relatively low values of R . *As such, given a BS coverage radius R , it is important to select the correct number of users in a cluster to ensure channel distinctness.* Finally, it can be observed that the perfect SIC can improve the performance of NOMA

significantly. Therefore, it is crucial to design efficient SIC strategies.

B. Impact of the Intensity of BSs

Fig. 4 depicts the average rate coverage of \bar{c} users in a NOMA representative cluster as a function of the maximum cell/cluster radius R with $\lambda_m|A| = 8$. The results are compared with the mean rate coverage of \bar{c} users in an equivalent OMA system where one user transmits at a time in each cell/cluster. The general conclusions and trends remain the same as in Fig. 3. However, it can be seen that increasing the intensity of BSs reduces the coverage probability significantly. Further, in low-inter-cell interference scenarios (see Fig. 3), we have observed that the performance of NOMA remains intact for increasing values of R . On the contrary, at high intensity of BSs, Fig. 4 shows that the NOMA performance degrades with increasing R . The reason is that the increasing values of R produce higher inter-cell interference as the users of neighboring cells are likely to be closer to the representative BS. Note that the degradation of OMA is caused by both the path-loss degradation as well as inter-cell interference, whereas in NOMA the degradation is mainly due to the increase of inter-cell interference. Finally, it can be seen that the rate coverage with imperfect SIC is least affected by the increasing intensity of BSs as the performance is limited by mainly the intra-cell interferences.

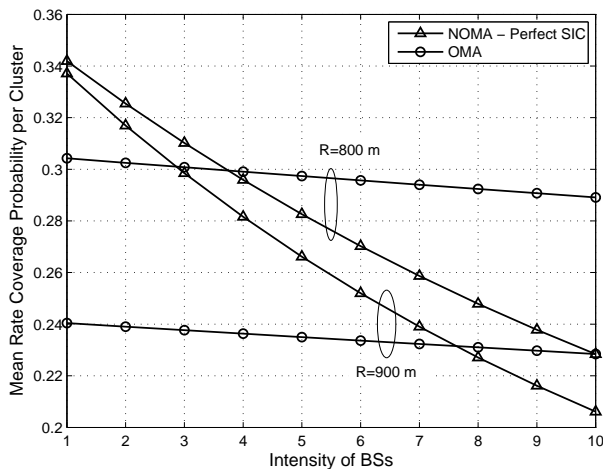


Fig. 5: Mean rate coverage probability as a function of $\lambda_m|A|$ in single-tier cellular network, $R_{th} = 1.5$ bps/Hz, $\bar{c} = 8$.

Fig. 5 demonstrates that increasing the intensity of BSs (or NOMA clusters) sharply degrades the performance of NOMA when compared to OMA. The reason is that several users transmit in each NOMA cluster at the same time. On the other hand, there is only one user transmitting per BS in OMA; thus the performance of OMA is relatively less prone to the increasing intensity of BSs. On the other hand, the performance of OMA decays significantly with the increase in R due to path-loss degradation, whereas in

NOMA, the degradation is not significant as is also evident from Fig. 3 and Fig. 4. As such, *NOMA can potentially outperform OMA for a higher intensity of BSs if the coverage radius of BSs can be increased to ensure channel distinctness.*

C. Analytical validation

Fig. 3 and Fig. 4 depict the mean rate coverage of \bar{c} users in a cluster as a function of the maximum cell/cluster radius R with $\lambda_m|A| = 2$ and $\lambda_m|A| = 8$, respectively. The impact of the distance approximation and the bound on the inter-cluster interference can be observed. The mismatch between the analysis and Monte-Carlo simulations is observed to increase with λ_m which shows that the mismatch is greatly contributed by the bound on the Laplace transform of the inter-cluster interference. Also, the impact of the inter-cluster interference bound is more visible for OMA as the rate coverage expression of OMA depends mainly on the inter-cluster interference.

D. Impact of the Desired User Rate Requirements

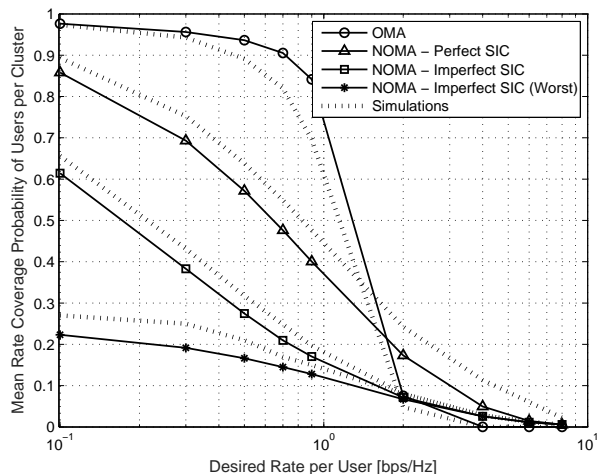


Fig. 6: Mean rate coverage probability as a function of the radius of each cluster in the single-tier cellular network, $\lambda_m|A| = 8$.

Fig. 6 depicts the mean rate coverage probability of all users in a NOMA cluster as a function of the users' rate requirements R_{th} considering perfect SIC, imperfect SIC, and worst-case SIC. The results are compared with the mean rate coverage of an equivalent OMA system in which one user transmits at a time in each cell/cluster. The performance of NOMA generally turns out to be better than OMA for higher values of R_{th} . The reason is that OMA is more susceptible to higher values of R_{th} due to the multiplicative factor $R_{\text{th}}\bar{c}$ in the SINR threshold of OMA. Note that $\gamma_m^{(\text{oma})} = 2^{R_{\text{th}}\bar{c}} - 1$. Interestingly, it can be seen that the rate coverage of worst-case SIC bound is quite similar to the imperfect SIC at

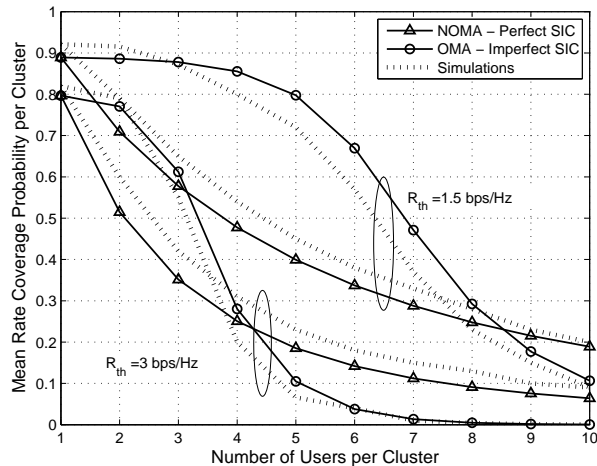


Fig. 7: Mean rate coverage probability as a function of the number of users per cluster in the single-tier cellular network, $\lambda_m|A| = 8$, $R = 0.8$ km.

higher values of R_{th} . However, the difference is visible at lower values of R_{th} . The reason is that, at lower values of R_{th} , the rate outages with imperfect SIC occur mainly due to the detection failures. As such, precisely mapping the impact of detection failures becomes crucial. Since the worst-case SIC bound assumes successful rate coverage of m -th user only when all relatively stronger users detected correctly, its worst performance is self-explanatory in this case.

E. Impact of the Number of Users per Cluster

Fig. 7 represents the mean rate coverage probability of a cluster as a function of \bar{c} considering $\lambda_m|A| = 8$. It can be seen that the rate coverage of both OMA and NOMA generally decreases with increasing \bar{c} and target rate requirements R_{th} of the users. Clearly, with increase in \bar{c} , the reduction is due to the increasing intra-cell and inter-cell interferences in NOMA and the reduced share of resources in OMA. On the other hand, with increasing R_{th} , the SINR threshold increases exponentially which reduces the coverage probability for both OMA and NOMA. However, the rate of decay of OMA is faster than NOMA for increasing R_{th} . The reason is that the SINR threshold of OMA has a multiplicative factor $R_{th}\bar{c}$ which is not the case in NOMA.

F. Poisson Point Process vs Poisson Cluster Process

Fig. 8 compares the performances of OMA and NOMA systems while comparing the two modeling approaches with equal intensity of BSs and users available in a square region. It is observed that PPP-based modeling shows reduced coverage probabilities for both OMA and NOMA systems, compared to PCP-based modeling. The reason is that there is no clustering of users around the BSs and they are

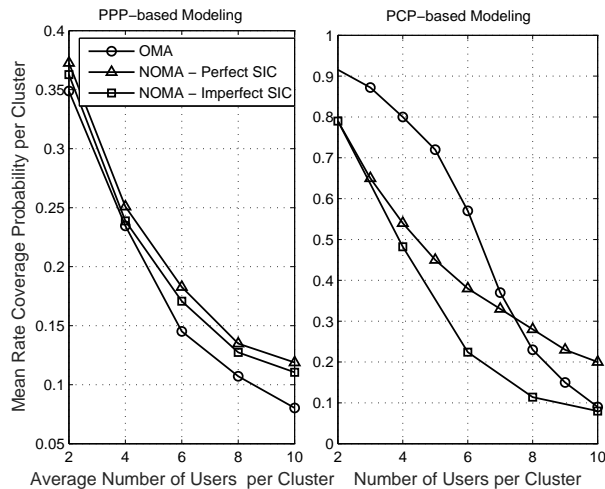


Fig. 8: Mean rate coverage probability as a function of the number of users per cluster for PCP-based modeling and total number of users as $\bar{c} * \lambda_m$ in the single-tier cellular network, $\lambda_m = 8$, $R = 800$ m, and $R_{th} = 1.5$ bps/Hz.

spread independent of the locations of the BSs. As such, the impact of path-loss degradation is significant. Note that we assume minimum distance-based association for PPP-based modeling. Also, the path-loss degradation is significant in PPP which benefits NOMA over OMA by lowering intra-cell interference among users. Consequently, NOMA with both perfect and imperfect SIC is observed to perform nearly the same and better than OMA. On the other hand, the PCP-based modeling shows that NOMA outperforms OMA for a certain range of users per cluster and that the perfect SIC outperforms imperfect SIC.

VII. CONCLUSION

We characterize the rate coverage probability of a user in NOMA cluster who is at rank m among all users and the mean rate coverage probability of all users in the cluster considering perfect SIC, imperfect SIC, and imperfect worst case SIC. In order to characterize the Laplace transforms of the intra-cluster interferences in closed-form considering both perfect and imperfect SIC scenarios, we derived novel distance distributions. The Laplace transform of the inter-cluster interference is then characterized by exploiting distance distributions from geometric probability as well as deriving an upper bound on the Laplace transform. Numerical results have been presented to validate the derived expressions. It has been shown that the average rate coverage of a NOMA cluster outperforms its counterpart OMA cluster in the cases of higher number of users per cell and higher target rate requirements. A comparison of PPP-based and PCP-based modeling has been conducted and it has been shown that the PPP-based modeling provides optimistic results for the NOMA systems. Also, the distinctness of perfect and imperfect SIC is difficult to calibrate with PPP-based modeling of NOMA systems.

APPENDIX A
PROOF OF LEMMA 1

Given the cluster members (users) are ranked according to their distances from the cluster center (BS), the distance distribution of a user at rank m can be given using the standard theory of order statistics as follows [27]:

$$f_{r(m)}(r) = \frac{\bar{c}!(F_r(r))^{m-1}(1 - F_r(r))^{\bar{c}-m}f_r(r)}{(\bar{c} - m)!(m - 1)!}. \quad (\text{A.1})$$

For a Matern cluster process, cluster members are uniformly and identically distributed around their respective cluster center (BS); therefore, the unordered probability density function (PDF) and cumulative density function (CDF) of their distances from the cluster center is given by (2) and r^2/R^2 , respectively. As such, (A.1) can be rewritten as:

$$f_{r(m)}(r) = \frac{\bar{c}!(\frac{r^2}{R^2})^{m-1}(1 - \frac{r^2}{R^2})^{\bar{c}-m}(\frac{2r}{R^2})}{(\bar{c} - m)!(m - 1)!}. \quad (\text{A.2})$$

Using the definition of Gamma function $\Gamma(x) = (x - 1)!$, the definition of the Euler Beta function $B(p, q) = \frac{\Gamma(p)\Gamma(q)}{\Gamma(p+q)}$, and doing some algebraic manipulations, we can write (A.2) as:

$$f_{r(m)}(r) = \frac{2\frac{r^{2m-1}}{R^{2m}}(1 - \frac{r^2}{R^2})^{\bar{c}-m}}{B(m, \bar{c} - m + 1)}. \quad (\text{A.3})$$

Now using the definition of the Generalized Beta (GB) distribution for a random variable Z , i.e.,

$$f_Z(z) = \frac{|a|z^{ap-1}(1 - (1 - c)(z/b)^a)^{q-1}}{b^{ap}\mathcal{B}(p, q)(1 + c(z/b)^a)^{p+q}}, \quad 0 \leq z^a \leq \frac{b^a}{1 - c},$$

and substituting $c = 0$, $z = r$, $a = 2$, $b = R$, $p = m$, and $q = \bar{c} - m + 1$, the result in **Lemma 1** can be readily proved. Note that the GB distribution with $c = 0$ becomes a GB distribution of the first kind.

APPENDIX B
PROOF OF LEMMA 2

The joint distribution of the distances of the users in $\mathcal{N}_{\text{out}}^{x_0} \in \{m+1, m+2, \dots, \bar{c}\}$, i.e., $f_{r(m+1), r(m+2), \dots, r(\bar{c})}$ can be derived along the lines of [13] as follows:

$$\begin{aligned} &\stackrel{(a)}{=} \bar{c}! \prod_{i=m}^{\bar{c}} f_r(r(i)) \int \cdots \int \prod_{i=1}^{m-1} f_r(r(i)) dr_{(1)} \cdots dr_{(m-1)}, \\ &\stackrel{(b)}{=} \frac{\bar{c}!}{(m-1)!} \prod_{i=m}^{\bar{c}} f_r(r(i)) \left(\int_0^{r(m)} f_r(r) dr \right)^{m-1}, \\ &= \frac{\bar{c}!}{(m-1)!} \prod_{i=m}^{\bar{c}} f_r(r(i)) (F_r(r(m)))^{m-1}, \end{aligned} \quad (\text{B.1})$$

where (a) follows from averaging out the distance variables $r_{(1)}, r_{(2)}, \dots, r_{(m-1)}$ and (b) follows from the i.i.d. property. Now given the distance $r_{(m)} = \hat{r}$, the conditional joint distribution of the distances of the users in $\mathcal{N}_{\text{out}}^{x_0} \in \{m+1, m+2, \dots, \bar{c}\}$, i.e., $f_{r_{(m+1)}, r_{(m+2)}, \dots, r_{(\bar{c})} | r_{(m)}}(r_{(m+1)}, r_{(m+2)}, \dots, r_{(\bar{c})} | r_{(m)})$ can be given as follows:

$$(\bar{c} - m)! \prod_{i=m+1}^{\bar{c}} \frac{f_r(r_{(i)})}{1 - F_r(r_{(m)})}, \quad r_{(m)} \leq r_{(i)}. \quad (\text{B.2})$$

It is noteworthy that, for perfect SIC scenario, the interference experienced at the BS from users in set $\mathcal{N}_{\text{out}}^{x_0}$ is cumulative therefore the interfering users can be chosen without any specific ordering. Subsequently, the permutation $(\bar{c} - m)!$ in (B.2) will not appear and the conditional joint distribution of the unordered set of distance random variables is given as:

$$f_{r_{m+1}, \dots, r_{\bar{c}} | \hat{r}}(r_{m+1}, \dots, r_{\bar{c}} | \hat{r}) = \prod_{i=m+1}^{\bar{c}} \frac{f_r(r_i)}{1 - F_r(r_{(m)})}, \quad (\text{B.3})$$

where $r_{(m)} \leq r_i$. Consequently, the product of truncated distributions in (B.3) implies that the random variables of the unordered set are i.i.d. Therefore, the distribution of $m - 1$ i.i.d. distance variables can be given as in **Lemma 2**. Using similar arguments, the conditional PDF of r_{in} can be derived.

APPENDIX C

PROOF OF LEMMA 4

The Laplace transform of the intra-cluster interference with perfect SIC as defined in (19), can be derived as follows:

$$\begin{aligned} \mathcal{L}_{I_{\text{intra}}^m}(s) &= \mathbb{E} \left[\exp \left(-s \sum_{y \in \mathcal{N}_{\text{out}}^{x_0}} P_u h_{y x_0} \|y\|^{-\alpha} \right) \right], \\ &= \mathbb{E}_{\mathcal{N}_{\text{out}}^{x_0}} \left[\prod_{y \in \mathcal{N}_{\text{out}}^{x_0}} \mathbb{E}_{h_{y x_0}} \left[\exp \left(-s P_u h_{y x_0} \|y\|^{-\alpha} \right) \right] \right], \\ &\stackrel{(a)}{=} \mathbb{E}_{\mathcal{N}_{\text{out}}^{x_0}} \left[\prod_{y \in \mathcal{N}_{\text{out}}^{x_0}} \frac{1}{1 + s P_u \|y\|^{-\alpha}} \right], \\ &\stackrel{(b)}{=} \left(\int_{\hat{r}}^R \frac{1}{1 + s P_u r_{\text{out}}^{-\alpha}} f_{r_{\text{out}} | \hat{r}}(r_{\text{out}} | \hat{r}) dr_{\text{out}} \right)^{\bar{c} - m}. \end{aligned}$$

Note that (a) follows from the definition of the Laplace transform of $h_{y x_0}$ which is exponentially distributed unit mean random variable and (b) follows from the conversion of Cartesian to polar coordinates as well as the fact that the distances from the interfering devices in set $\mathcal{N}_{\text{out}}^{x_0}$ to the BS, conditioned on \hat{r} , are

i.i.d. random variables. The integral in (b) can be solved in closed-form as follows:

$$\frac{R^{2+\alpha} {}_2F_1\left[1, 1 + \frac{2}{\alpha}, 2 + \frac{2}{\alpha}, -\frac{R^\alpha}{sP_u}\right] - \hat{r}^{2+\alpha} {}_2F_1\left[1, 1 + \frac{2}{\alpha}, 2 + \frac{2}{\alpha}, -\frac{\hat{r}^\alpha}{sP_u}\right]}{s(P_u/2)(\alpha+2)(R^2 - \hat{r}^2)}. \quad (\text{C.4})$$

Finally, **Lemma 3** can be readily obtained after simplifying the Gauss hyper-geometric functions in (C.4) as ${}_2F_1[a, b, b+1, z] = bz^{-b}\mathbf{B}_z(b, 1-a)$ [28, Eq. 07.23.03.0084.01] and then using the definition of the Generalized incomplete Beta function as $\tilde{\mathbf{B}}_{z_1, z_2}(x, y) = \mathbf{B}_{z_2}(x, y) - \mathbf{B}_{z_1}(x, y)$.

APPENDIX D

PROOF OF LEMMA 5

The Laplace transform of the intra-cluster interference experienced by the transmission of user at rank m , as defined in (9), can be derived as follows:

$$\begin{aligned} \mathcal{L}_{\text{add}}^m(s) &= \mathbb{E} \left[\exp \left(-s \sum_{y(j) \in \mathcal{N}_{\text{in}}^{x_0}} (1 - b(j)) P_u h_{y_{x_0}} \|y(j)\|^{-\alpha} \right) \right], \\ &\stackrel{(a)}{=} \mathbb{E}_{\mathcal{N}_{\text{in}}^{x_0}} \left[\prod_{y(j) \in \mathcal{N}_{\text{in}}^{x_0}} \mathbb{E}_{h_{y_{x_0}}} [e^{-s(1-b(j))P_u h_{y_{x_0}} \|y(j)\|^{-\alpha}}] \right], \\ &\stackrel{(b)}{=} \mathbb{E}_{\mathcal{N}_{\text{in}}^{x_0}} \left[\prod_{y(j) \in \mathcal{N}_{\text{in}}^{x_0}} \left(\frac{1}{1 + s(1-b(j))P_u \|y(j)\|^{-\alpha}} \right)^{1-b(j)} \right], \\ &\stackrel{(c)}{=} \prod_{j=1}^{m-1} \left(\int_0^{\hat{r}} \frac{1}{1 + sP_u r^{-\alpha}} f_{r(j)}(r(j)|\hat{r}) dr(j) \right)^{1-b(j)}, \end{aligned} \quad (\text{D.5})$$

where (a) follows by applying the properties of the exponential function, (b) follows from the Laplace transform of $h_{y_{x_0}}$ which is exponentially distributed unit mean random variable and by shifting the term $1 - b(j)$ into the powers. Note that $b(j) \in \{0, 1\}$ and if $b(j) = 1$ the interference from i -th ranked user is absent as its signal gets detected and if $b(j) = 0$ the interference from j -th ranked user is present since its signal goes undetected, Finally, (c) follows from the conversion to polar coordinates and exploiting the following assumption.

Assumption: Note that the distributions of ranked user devices in set $\mathcal{N}_{\text{in}}^{x_0}$ are correlated. The dependence is however weak since they are multiplied with random fading channel gains [29]. Thus, we ignore this dependence and subsequently interchange the operation of products and integration.

Finally, substituting the distributions from Lemma 3, we apply the Binomial expansion and solve the integral using [28, Eq. 07.23.03.0084.01] to obtain **Lemma 5**.

APPENDIX E

PROOF OF LEMMA 6

By applying the McLaurin Series expansion $\sin^{-1}(z) = \sum_{k=0}^{\infty} \frac{\Gamma[k+0.5]}{\sqrt{\pi}(2k+1)k!} z^{2k+1}$ and the Binomial expansion, I_2 can be solved in closed-form as follows:

$$\sum_{k=0}^{\infty} \sum_{j=0}^{2k+1} \frac{C \tilde{\mathbf{B}}\left(\frac{-(v-R)^\alpha}{s}, \frac{-(v+R)^\alpha}{s}, 1 + \frac{4-2j+2k}{\alpha}, 0\right)}{\alpha R^2 (-1/s)^{\frac{4-2j+2k}{\alpha}}} - \frac{\tilde{\mathbf{B}}\left(\frac{-(v-R)^\alpha}{s}, \frac{-(v+R)^\alpha}{s}, 1 + \frac{3}{\alpha}, 0\right)}{\alpha R^2 s^{-\frac{3}{\alpha}} (-1/s)^{\frac{3}{\alpha}}}, \quad (\text{D.6})$$

where $C = \frac{\Gamma[k+0.5] \binom{2k+1}{j}}{\sqrt{\pi}(2k+1)k!(v^2-R^2)^{-j} v^{2k+1} 2^{2k}}$. Similarly, the first part of I_1 can be given in closed-form as $\frac{2\mathbf{B}\left(-\frac{(R-v)^\alpha}{s}, 1 + \frac{2}{\alpha}, 0\right)}{(-1/s)^{1+\frac{2}{\alpha}} \alpha (R^2)s}$ and second part of I_1 can be solved in closed-form by replacing $v - R$ with $R - v$ in (D.6). Interested readers can go through [26] for further details.

REFERENCES

- [1] Y. Saito, Y. Kishiyama, A. Benjebbour, T. Nakamura, A. Li, and K. Higuchi, "Non-orthogonal multiple access (NOMA) for cellular future radio access," in *Proc. of IEEE Vehicular Technology Conference (VTC Spring)*, June. 2013.
- [2] A. Benjebbour, K. Saito, A. Li, Y. Kishiyama, and T. Nakamura, "Non-orthogonal multiple access (noma): Concept, performance evaluation and experimental trials," in *Proc. of IEEE International Conference on Wireless Networks and Mobile Commun. (WINCOM'15)*, Oct. 2015.
- [3] Z. Ding, Z. Yang, P. Fan, and H. Poor, "On the performance of non-orthogonal multiple access in 5G systems with randomly deployed users," *IEEE Signal Processing Letters*, vol. 21, no. 12, pp. 1501–1505, Dec. 2014.
- [4] Z. Ding, M. Peng, and H. V. Poor, "Cooperative non-orthogonal multiple access in 5G systems," *IEEE Commun. Letters*, vol. 19, no. 8, pp. 1462–1465, Aug. 2015.
- [5] Y. Liu, Z. Ding, M. Elkashlan, and H. V. Poor, "Cooperative non-orthogonal multiple access with simultaneous wireless information and power transfer," *IEEE Journal of Selected Areas in Commun.*, vol. 34, no. 4, pp. 938–953, 2016.
- [6] Z. Ding, P. Fan, and H. V. Poor, "Impact of user pairing on 5g non-orthogonal multiple access downlink transmissions," *IEEE Trans. on Vehicular Technology*, vol. PP, no. 99, pp. 938–953, 2016.
- [7] N. Zhang, J. Wang, G. Kang, and Y. Liu, "Uplink non-orthogonal multiple access in 5g systems," *IEEE Commun. Letters*, vol. 20, no. 3, pp. 458–461, Mar. 2016.
- [8] T. Takeda and K. Higuchi, "Enhanced user fairness using nonorthogonal access with SIC in cellular uplink," in *Proc. IEEE VTC 2011-Fall*, Sep. 2011.
- [9] Y. Endo, Y. Kishiyama, and K. Higuchi, "Uplink Non-orthogonal Access with MMSE-SIC in the Presence of Inter-cell Interference," in *Proc. IEEE ISWCS*, 2012.
- [10] C. W. Sung and Y. Fu, "A game-theoretic analysis of uplink power control for a non-orthogonal multiple access system with two interfering cells," in *Proc. IEEE VTC 2016-Spring*, 2016.
- [11] H. Tabassum, M. S. Ali, E. Hossain, M. J. Hossain, and D.-I. Kim, "Non-orthogonal multiple access (noma) in cellular uplink and downlink: Challenges and enabling techniques," *arXiv:1608.05783*, 2016.
- [12] R. K. Ganti and M. Haenggi, "Interference and outage in clustered wireless ad hoc networks," *IEEE Trans. on Info. Theory*, vol. 55, no. 9, p. 40674086, Sep. 2009.
- [13] M. Afshang, H. S. Dhillon, and P. H. J. Chong, "Modeling and performance analysis of clustered device-to-device networks," *IEEE Transactions on Wireless Communications*, vol. 15, no. 7, pp. 4957 – 4972, July 2016.

- [14] M. Afshang, H. S. Dhillon, and P. H. J. Chong, "Fundamentals of cluster-centric content placement in cache-enabled device-to-device network," *IEEE Transactions on Communications*, vol. 64, no. 6, pp. 2511–2526, 2016.
- [15] Y. J. Chun, M. O. Hasna, and A. Ghayeb, "Modeling heterogeneous cellular Networks Interference Using Poisson Cluster Processes," *IEEE Journal on Selected Areas in Communications*, vol. 33, no. 10, pp. 2182 – 2195, Oct. 2015.
- [16] Chiranjib Saha, Harpreet S. Dhillon, "Downlink coverage probability of K-tier HetNets with general non-uniform user distributions," in *proc. IEEE ICC Kuala Lumpur, Malaysia*, 2016.
- [17] H. ElSawy and E. Hossain, "On stochastic geometry modeling of cellular uplink transmission with truncated channel inversion power control," *IEEE Trans. on Commun.*, vol. 13, no. 8, p. 44544469, Aug. 2014.
- [18] H. S. Dhillon, R. K. Ganti, F. Baccelli, and J. G. Andrews, "Modeling and analysis of K-tier downlink heterogeneous cellular networks," *IEEE Journal on Sel. Areas in Commun*, vol. 30, no. 3, p. 550 – 560, Apr. 2012.
- [19] Q. Ying, Z. Zhao, Y. Zhou, R. Li, X. Zhou, and H. Zhang, "Characterizing spatial patterns of base stations in cellular networks," in *Proc. IEEE ICC, Shanghai, China*, p. 490495, Oct. 2014.
- [20] M. Mollanoori and M. Ghaderi, "Fair and efficient scheduling in wireless networks with successive interference cancellation," *IEEE Wireless Communications and Networking Conference*, pp. 221–226, 2011.
- [21] C. Ma, W. Wu, Y. Cui, and X. Wang, "On the performance of successive interference cancellation in d2d-enabled cellular networks," *2015 IEEE Conference on Computer Communications (INFOCOM)*, pp. 37–45, 2015.
- [22] G. Geraci, M. Wildemeersch, and T. Q. S. Quek, "Energy Efficiency of Distributed Signal Processing in Wireless Networks: A Cross-Layer Analysis," *IEEE Transactions on Signal Processing*, vol. 64, no. 4, pp. 1034 – 1047, Feb. 2016.
- [23] M. Afshang and H. S. Dhillon, "Optimal geographic caching in finite wireless networks," in *Proc. IEEE SPAWC*, 2016.
- [24] M. Afshang and H. S. Dhillon, "Fundamentals of modeling finite wireless networks using Binomial point process," <https://arxiv.org/abs/1606.04405>, July 2016.
- [25] F. Adelantado, J. Prez-Romero, and O. Sallent, "Nonuniform traffic distribution model in reverse link of multirate/multiservice wcdma-based systems," *IEEE Transactions on Vehicular Technology*, vol. 56, no. 5, p. 29022914, Sep. 2007.
- [26] H. Tabassum, Z. Dawy, E. Hossain, and M. -S. Alouini, "Interference statistics and capacity analysis for uplink transmission in two-tier small-cell networks: A geometric probability approach," *IEEE Transactions on Wireless Communications*, vol. 13, no. 7, pp. 3837–3852, Mar. 2014.
- [27] H. A. David and H. N. Nagaraja, "Order Statistics," *3rd edition, New York: Wiley*, 2003.
- [28] Wolfram Research, *Mathematica Edition: Version 8.0*. Champaign, Illinois: Wolfram Research, Inc., 2010.
- [29] H. Tabassum, E. Hossain, M. J. Hossain, and D. I. Kim, "On the spectral efficiency of multiuser scheduling in rf-powered uplink cellular networks," *IEEE Transactions on Wireless Communications*, vol. 14, no. 7, pp. 3586–3600, 2015.